Sigma Journal of Engineering and Natural Sciences
Web page info: https://sigma.yildiz.edu.tr
DOI: 10.14744/sigma.2023.00130

Research Article

Experimental investigation and FEM analysis of chip morphology in the turning of ASTM F-75 CoCrMo alloy

Ender EMİR[1,*], Burak ÖZDEMİR[2], Erkan BAHÇE[3]

[1]Elbistan Vacational School, Istiklal University, Kahramanmaraş, 46300, Türkiye
[2]Hekimhan MES Vacational School, Malatya Turgut Ozal University, Malatya, 44210, Türkiye
[3]Department of Mechanical Engineering, Inonu University, Malatya, 44280, Türkiye

ARTICLE INFO

Article history
Received: 13 October 2022
Revised: 29 November 2022
Accepted: 16 June 2023

Keywords:
ASTM-F75 CoCrMo Alloy; Chip Morphology Modelling; FEM; Turning

ABSTRACT

During the machining process, problems such as tool wear, high temperature, force distribution, and surface quality deterioration must be fully understood. Control of these problems with experimental studies and numerical analyses is important in ensuring dimensional accuracy and surface integrity of the cutting tool, workpiece, and also the finished product. The aim of this study is to investigate the effects of machining parameters on chip morphology, residual stresses and tool wear in turning operations of ASTM-F75 CoCrMo alloy experimentally and by finite element method (FEM) simulation. The study was carried out at three different feed rates (0.1, 0.2, 0.3 mm/rev) and at a constant cutting speed of 80 m/min both experimentally on a CNC turning machine and with FEM simulation. From the obtained results, the formation of cracks and adhesions on the surfaces of the chip were observed due to the increase of the feed rate. According to the orthogonal cutting model, chip height ratio (Gs) and tooth pitch (Pc) values of saw-tooth chips supported each other with measurements taken from both FEM images and experimental images. With the increase of the forward speed, the Gs ratio decreased, while the Pc increased. In addition, microscopic images obtained from the cutting tool also showed that the rate of crater wear gradually increased with increasing feed rate. As a result, it is seen that machining parameters have a significant effect on cutting tool and chip morphology in CoCrMo ASTM-F75 alloy turning.

Cite this article as: Emir E, Özdemir B, Bahçe E. Experimental investigation and FEM analysis of chip morphology in the turning of ASTM F-75 CoCrMo alloy. Sigma J Eng Nat Sci 2024;42(3):679–691.

INTRODUCTION

CoCrMo alloys are widely used in fracture bone joints, knee and hip prosthesis applications due to their high biocompatibility and mechanical properties. However, in addition to the high biocompatibility it provides, the high mechanical properties of the elements in the alloy can cause problems in the machining of the final product. One of these problems is tool wear and deterioration of surface

***Corresponding author.**
*E-mail address: ender.emir@istiklal.edu.tr

This paper was recommended for publication in revised form by Editor in-Chief Ahmet Selim Dalkilic

integrity due to the high temperature during chip removal. These problems that occur during the manufacturing process increase both the production time and cost. Therefore, it is very important to problems estimate and control any that may arise during fully production.

One of the most important issues examined in the literature on the machining of hard materials is tool wear [1-5]. Tool wear in machining has an economically important role in chip removal. Given that machining is a complex process, predicting tool wear is very difficult and complex. The turning of hard alloys such as CoCrMo rises to approximately 850-1200°C depending on the temperature processing parameters that occur between the tool and the workpiece. Therefore, knowledge of tool wear mechanisms and the ability to predict tool life are important in metal cutting. It should be noted that contact conditions and areas in the cutting zone also affect tool wear [6]. Determining these accurances by experimental studies affects important parameters such as processing time and cost. However, changes in parameters such as feed rate and cutting speed during the experiments especially affect the force distributions, heat generation and tool wear. The workpiece material and its physical properties affect the cutting force for the applied cutting conditions. The optimum performance of a cutting tool requires an accurate combination of machining parameters and cutting conditions [7]. The use of FEM software to determine the ideal conditions for chip removal is necessary for the optimization of experimental studies. Therefore, FEM software is important in the optimization of machining processes. Thanks to these softwares, it is possible to obtain various results such as cutting force, cutting temperature, stress, tool temperature, chip formation, and heat transfer when cutting. When the studies on this subject are examined in the literature, it is seen that numerical analyses performed in the FEM environment are similar to the experimentally obtained results [8,9].

On the other hand, the chips produced during the manufacturing process adversely affect the surface quality, tool wear, and the resulting forces of the final product. Tool wear and surface quality deterioration can be prevented by microscopic examination of the chips acquired as a result of the experiments. It is known in the literature that chip morphology resulting from the machining of hard alloys is commonly caused by adhesion and cracks. In addition, it is necessary to determine the surface and subsurface stresses for the detection of damaging effects such as wear, fatigue, fracture and collapse in the contact that occurs during machining. [10,11]. For this reason, studies have been carried out in the literature to investigate the effects of machining parameters on tool wear and chip morphology. Zhang et al. (2014) investigated the relationship between chip morphology and tool wear in ultra-precision raster milling (UPRM). A cutting experiment was performed to explore chip morphologies under different flank wear area widths. Theoretical and experimental results revealed that the occurrence of tool flank wear can cause cutting chips to be cut on both the cutting edge and reduce the length of the cutting chips in the feed direction [12]. Japtag et al. (2018) have worked on the chip formation mechanism in CNC turning of CoCrMo alloy [13]. They conducted experiments at different feed rate, cutting speed, and cutting depths. In the results they obtained, they stated that the chip thickness ratio increased due to the increase in the feed rate. Parida and Maity (2018) Monel-400 material was seen as a result of turning the microscope images saw the formation of saw tooth form [14]. They also stated that the rate of progress is an important parameter in the formation of continuous and discontinuous chips. Zhao et al. (2018) studied the effects of Ti6Al4V alloy on the chip by cryogenic turning [15]. During the cryogenic cutting process, with the increase of cutting speed, the chip height ratio and serrated pitch of titanium alloy chip increase. Tang et al. (2019) studied the tool wear performance in dry turning of AISI D2 steel at various hardness levels [5]. In the experimental results, they observed that lateral abrasions and crater abrasions occured significantly due to the increase in the hardness of the workpiece. Bolat et al. (2021) the processing properties of pumice reinforced AA7075 syntactic foams produced by sandwich infiltration technique were investigated by performing face turning at different cutting speeds (25, 50, and 100 m/min) and feed rates (0.05, 0.10, and 0.15 mm/rev). In the results they obtained, they said that the shape of the metal chips changed from long/continuous character to saw tooth morphology depending on the increasing cutting speed levels, while the pumice particles showed a tendency to break as their feed rate increased [16]. Pop and Titu (2021) investigated the effect of clearance angle change on chip formation in the turning process using FE analysis. As a result of their study, they said that with the increase of the radius of the cutting edge, the stress distribution is radial over a larger area of the part, and therefore the deformation of the chip is smaller [17]. Wakjira and Ramulu (2022) investigated the analysis of chip morphology using the FE method in the turning of CSN 12050 carbon steel with various tool geometries (tool rake and flank angles). In the experiments, rake angles of 0, 5, and 10, edge angles of 0 and 6, and depths of cut of 0.2 mm and 0.5 mm were determined using adaptive meshing for the tool. In the FE analysis results, they estimated increasing von Mises stresses and decreasing cutting forces with 10 rake angles and 6 edge angles [18]. Okokpujie et al. (2022) carried out an experimental study and FEM analysis to examine tool wear during turning of Al-Si-Mg alloy. In particular, they investigated the effect of process parameters and machining conditions on tool wear. They said that the depth of cut is the most effective process parameter in terms of tool wear [19].

The machining of ASTM-F75 CoCrMo alloy affects the dimensional accuracy deterioration and forces due to irregularities in chip removal and tool wear, creating extra costs to reach the desired standards. One of the factors affecting the yield of the product to be obtained in the chip removal process is sawdust. Therefore, it is important to examine the effect of machining parameters on chip formation. The aim of this study is to investigate the effects of different feed

rate increases on chip types, residual stresses and tool wear in the machining of CoCrMo material and to compare the results obtained with the FEM model. Unlike the literature, the effects of feed rate on chip morphology, residual stress, and the occurrence of tool wear are discussed together. In this context, the results obtained by turning operations at three different feed rates at a constant cutting speed and FEM results are presented together. Significant differences were observed in chip types, especially with the increase in feed rate. In addition, significant wear was observed in the cutting tool with the force and temperature distribution during the turning operation.

EXPERIMENTAL PROCEDURE

Experimentel Setup and FE Modelling

The results of the study were obtained by using two different methods. In the first method, machinig process was performed on turning machine at different feed rates (Figure 1). SEM images were taken of the chip and the cutting tool used as a result of the experiment. In the second method, chip removal simulation was performed by using ThirdWave software with FEM (Figure 1). As a result of this method, temperature changes and force distributions that occured in the cutting tool were obtained.

The chemical composition of the CoCrMo-F75 alloy used in the study is given in Table 1. The mechanical properties of the alloy are given in Table 2. The cutting process was made of tungsten carbide (WC) material with a 55° tool tip angle and a radius of 0.08 mm. In the study, the processing parameters are given in Table 3. In particular, the cutting speed was set low for tool and workpiece integrity. In addition, a mesh with a tetrahedral element type, an element size of 0.1 mm, 3517 nodes, and 10265 elements were used for FEM simulations. In order to analyze the analyses, linear motion was given to the cutting tool, while the workpiece was fixed. The Johnson-Cook material model was implemented for the flow stress of the workpiece and can be represented as Eq. (1)

$$\sigma = [A+B(\varepsilon)^n]\left[1+C\ln\left(\frac{\dot{\varepsilon}}{\dot{\varepsilon}_0}\right)\right]\left[1-\left(\frac{T-T_0}{T_m-T_0}\right)^m\right] \quad (1)$$

where σ is the flow stress, ε is the plastic strain, $\dot{\varepsilon}$ is the plastic strain rate and $\varepsilon \cdot 0$ is the reference plastic strain rate. T, Tr and Tm are the work temperature, reference temperature and material melting temperature, respectively. A, B, n, C and m are the material constants. The flow chart for FEM analysis is given in Figure 2.

Table 1. Chemical composition of CoCrMo [20]

Element	wt.%
Cr	26-30
Mo	5-7
C	≤0.14
Fe	0.75 (max)
Mn	1 (max)
Si	1 (max)
Ni	0.25 (max)
Co	Balance

Table 2. Mechanical properties of CoCrMo [21]

Young's Modulus (GPa)	220
Poisson Ratio (u)	0.29
Hardness (HRc)	35
Elongation (%)	14
Ultimate Tensile Strength (MPa)	1020
Yield Strength MPa	600

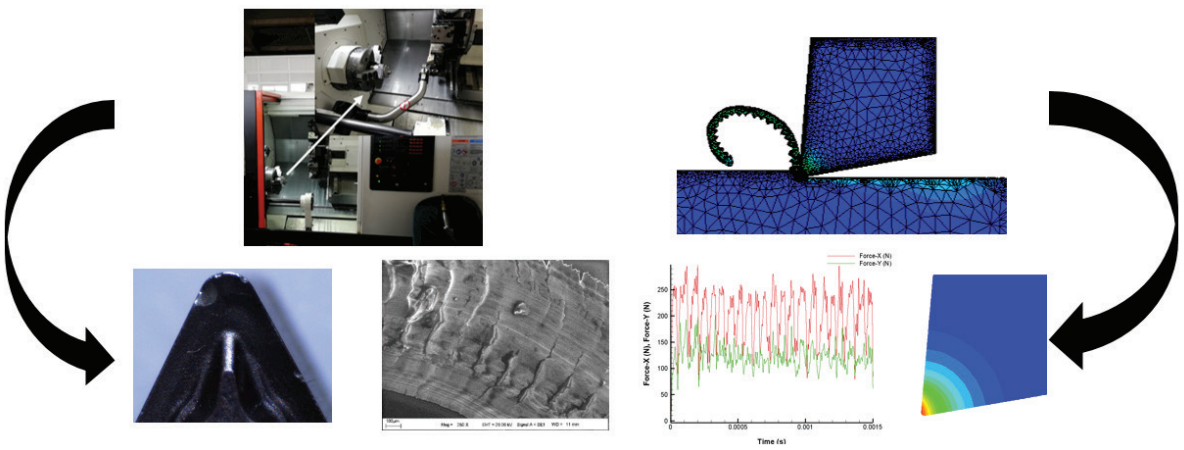

Figure 1. Machining procedure.

Table 3. Machining parameters of CoCrMo

Cutting speed (m/min)	Spindle speed (rpm)	Feed rate (mm/rev)	Cutting depth (mm)
80	150	0.1 0.2 0.3	0.5

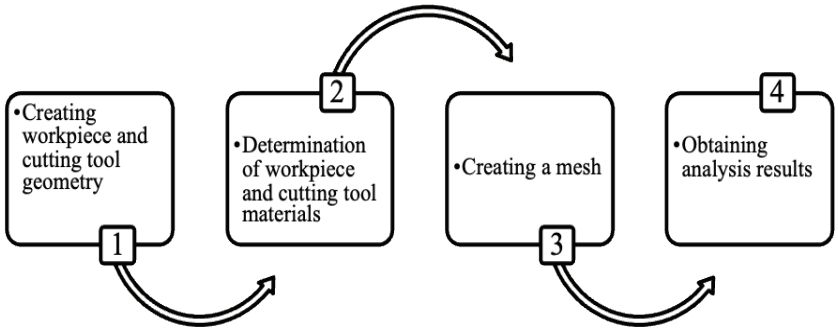

Figure 2. Machining parameters of CoCrMo.

RESULT AND DISCUSSION

Simulated Force and Temperature Distribution

Figure 3 shows the force changes resulting from a series of FEM simulations performed for three different feeds (0.1 mm/rev, 0.2 mm/rev, 0.3 mm/rev) at a constant cutting speed of 80 m/min. In the results obtained, it was seen that the force value in the X direction was highest at the feed rate of 0.3 mm/rev. Considering the force variation range, it was higher at a feed rate of 0.3 mm/rev than at a feed

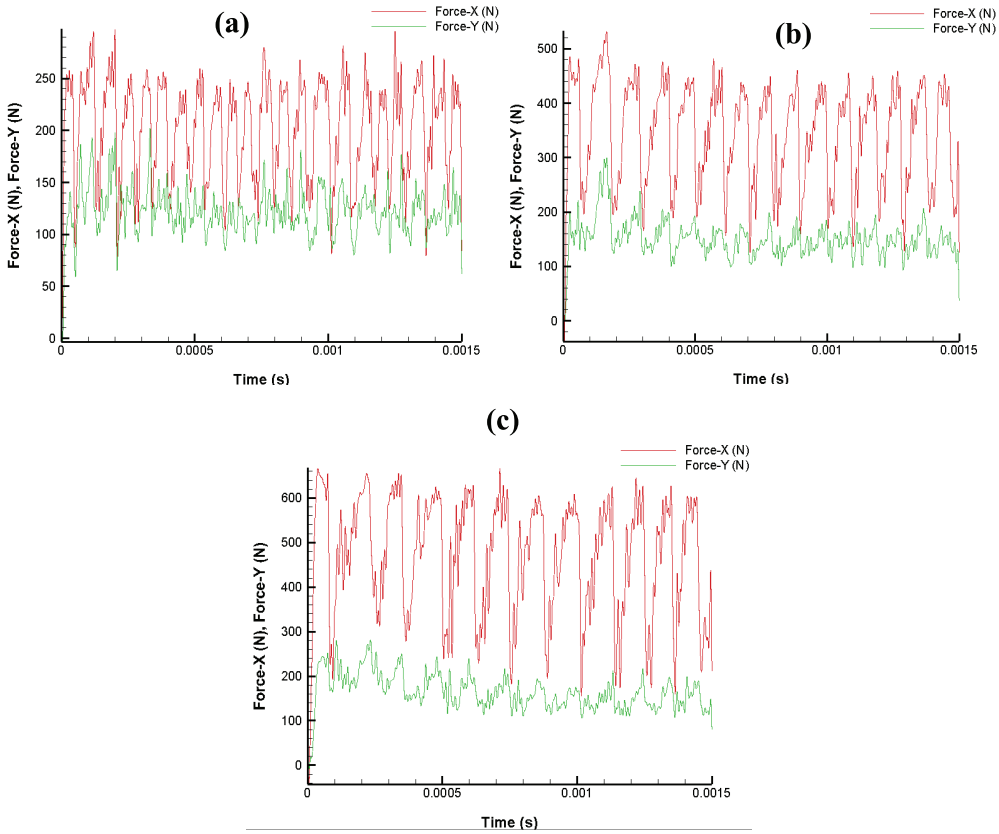

Figure 3. Force distribution during chip removal; a) 0.1 mm/rev, b) 0.2 mm/rev, c) 0.3 mm/rev.

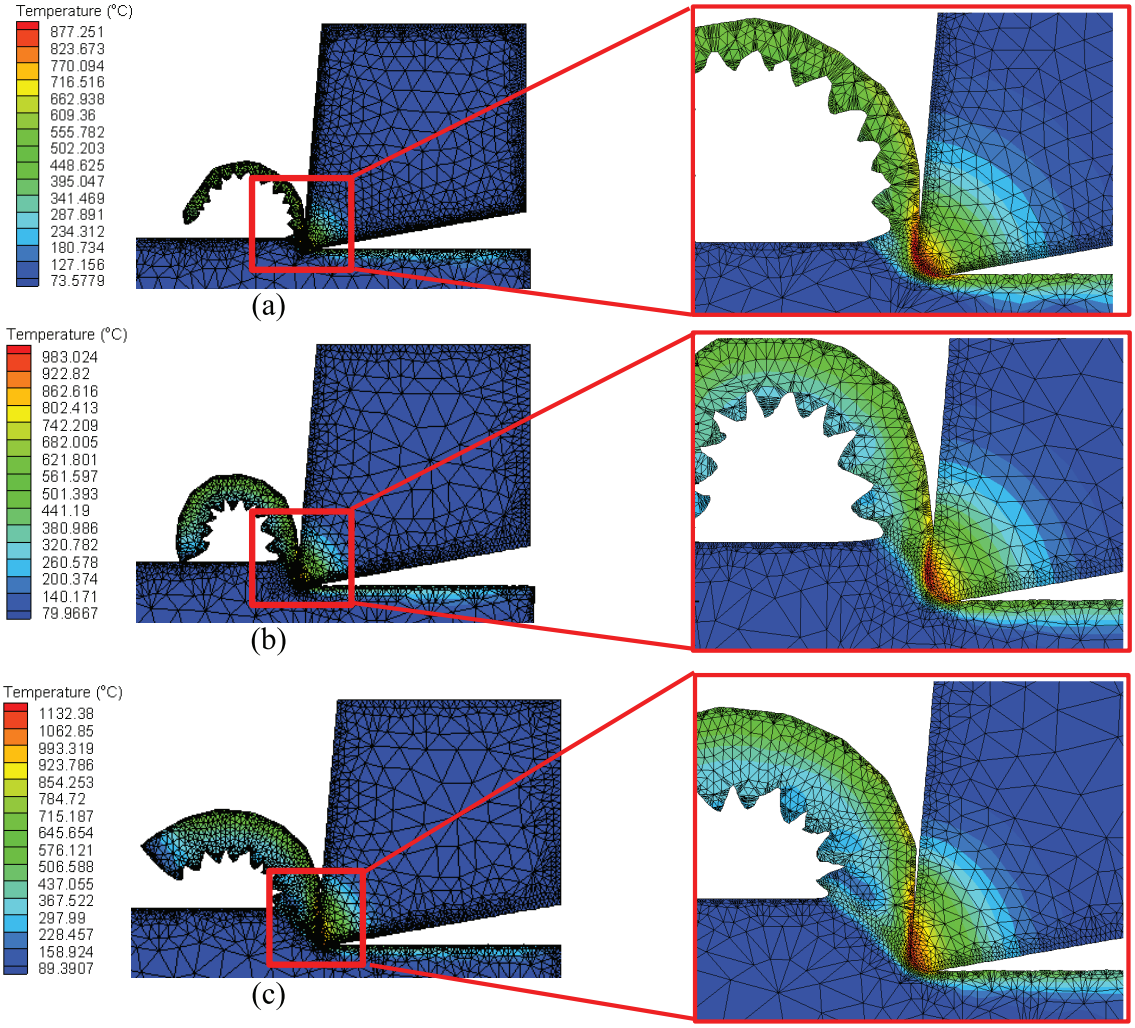

Figure 4. Temperature distribution during chip removal; a) 0.1 mm/rev, b) 0.2 mm/rev, c) 0.3 mm/rev.

rate of 0.2 and 0.1 mm/rev. Due to thermal softening, the heating effect reduces workpiece stability [14]. As a result of FEM analysis, the maximum temperatures were 877.25°C at 0.1 mm/rev, 983.024°C at 0.2 mm/rev, and 1132.38° C at 0.3 mm/rev (Figure 4). As a result of the FEM analysis, it was seen that the temperature increased with the increase of the feed rate. In this case, it was seen in the results of the analysis that the forces that occurred during cutting were effective.

Effect of Machining Parameters on Chip Morphology Characteristics

Figure 5 shows typical chip morphologies at different feed rates. The size of the chips was directly related to the feed rate. If the feed rate was 0.1 mm/rev, continuous chips were observed. On the other hand, discontinuous chips were observed at feed rates of 0.2 mm/rev and 0.3 mm/rev respectively. From the acquired results, it can be concluded that an increase in the feed rate facilitates discontinuous chip formation. This means that more chip thickness will be removed with increased feed during chip removal, resulting in the chips being broken down into smaller pieces instead of curling or striping.

Figure 6 shows SEM images of chip morphologies that occur at a constant 80 m/min of cutting speed at different feeds. In the obtained images, the surface of the chip was seen to be smooth at 0.1 mm/rev. At 0.2 mm/rev, it was observed that the chip surfaces caused cracks due to the increased heat generation during chip removal. A further feed rate of 0.3 mm/rev caused an increase in the amount of chips removed per unit feed, resulting in increased temperatures between the tool and the chip. As a result, it was observed that there was significant adhesion on the surface of the chip.

It is seen that chip-shaped saw-tooth formations occur due to the natural brittleness of the material when removing chips from the surfaces of hard materials [8]. Similar results were also seen from the performed FEM analysis (Figure 7). For detailed analysis of the effect of machining parameters on chip morphology, optical images from chip

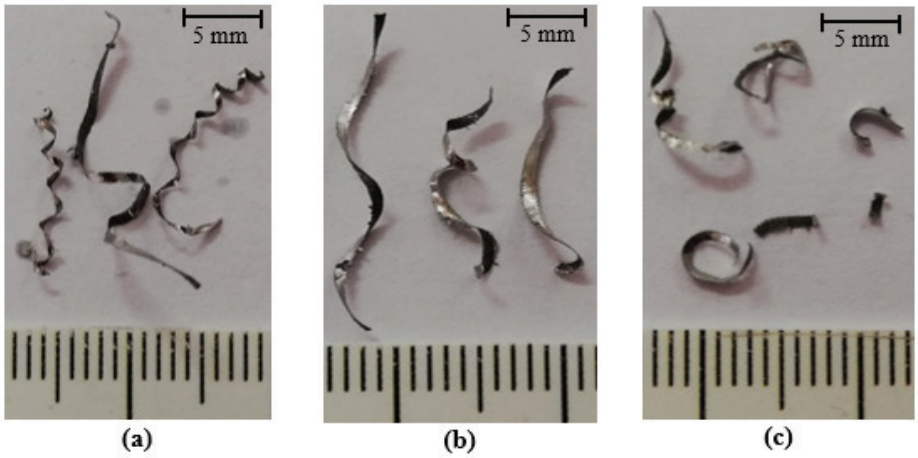

Figure 5. Chip images at a constant cutting speed of 80 m/min; a) 0.1 mm/rev, b) 0.2 mm/rev, c) 0.3 mm/rev.

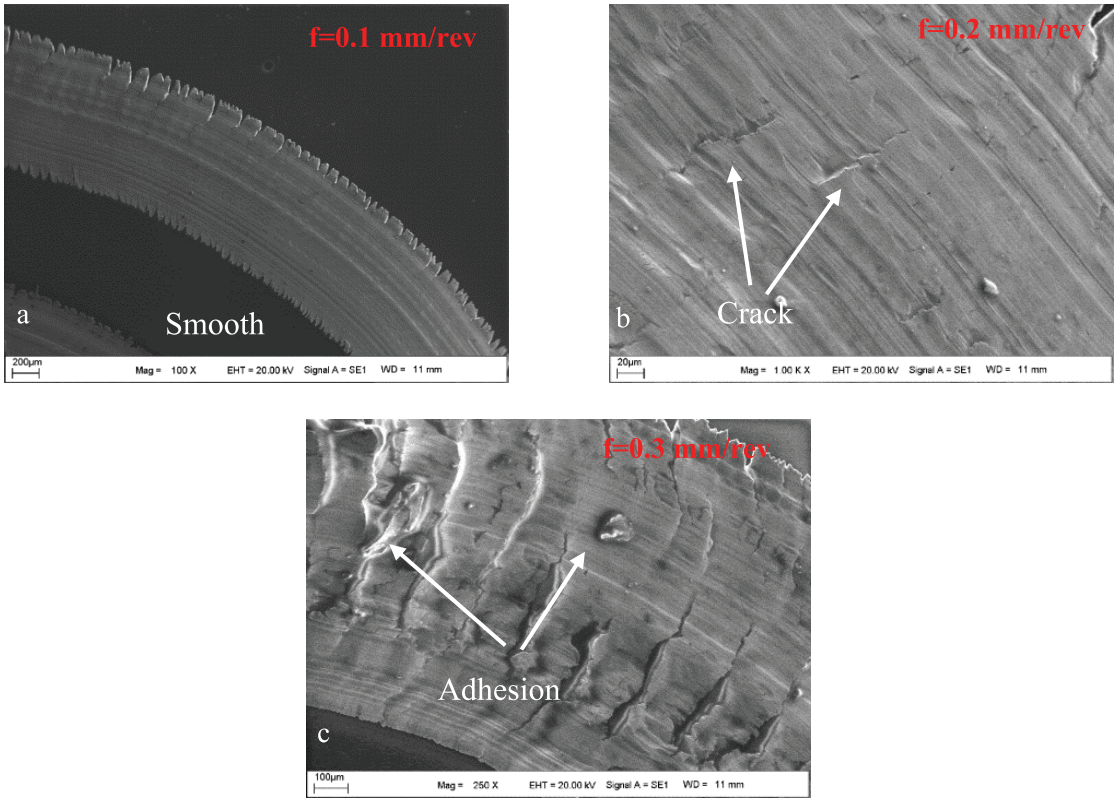

Figure 6. Chip SEM images: a) smooth, b) crack, c) adhesion.

surfaces are as shown in Figure 8. In the study, it was seen that saw-tooth structures were formed in chip morphology due to the increase in progress. This is explained by the localization of the stresses in the cutting zone during the turning of the alloy and the instability of the plastic flow of the workpiece material [12, 22]. In fact, in the FEM analysis formed according to the orthogonal cutting model, it was observed that a localized stress zone was formed in the primary deformation region during metal removal (Figure 9).

Chip morphologies are not uniform due to various feed rates. SEM images showed that lamellar structures were formed on the free surface of the chips (Figure 10). This type of structure extends along the width of the chips, which is normal to the chip flow direction. While the outer edges of the chips have saw-tooth structures, when the inner parts are examined, a transition to the lamellar structure is observed (Figure 10a). Saw-tooth structures are not clear in this region. The increase in the feed rate reveals the

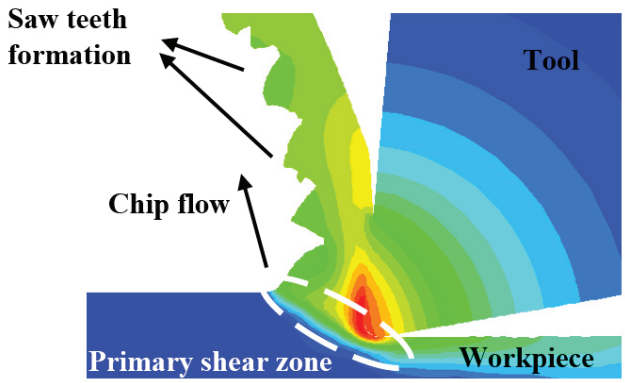

Figure 7. Saw tooth formation as a result of FEM analysis at 0.3 mm/rev.

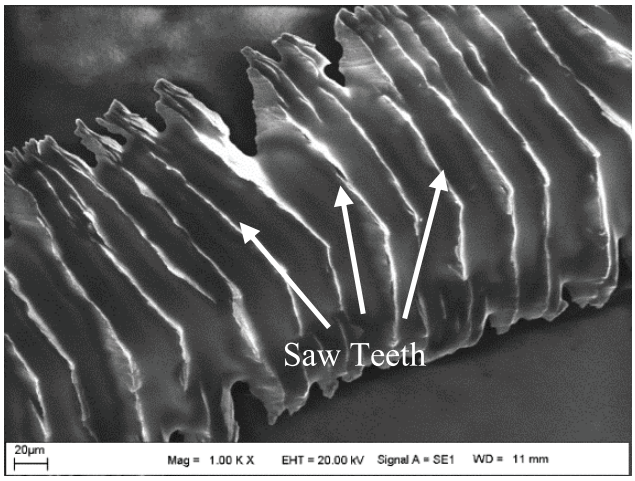

Figure 8. Saw tooth formation at 0.3 mm/rev.

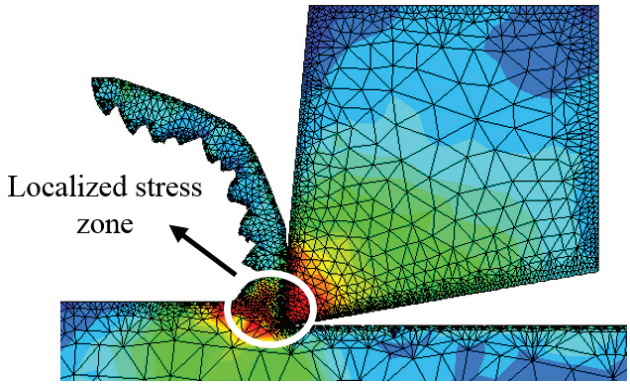

Figure 9. Localizated stress zone at 0.3 mm/rev.

formation of regular lamellar structure (Figure 10b, Figure 10c). This is due to the cutting band formed due to the high feed rate when the material in front of the cutting tool is moved in the cutting direction [23-25].

Figure 11 shows that the chip morphologies change significantly at different feed rates. Continuous chip formation is observed compared to the chips obtained at a low feed rate (f = 0.1 mm/rev) and other feed rates (f = 0.2 mm/rev and f = 0.3 mm/rev) (Figure 11a). With an increase in the feed rate, the chip increasingly scalloped on a takes shape (Figure 11b and Figure 11c). This is due to cyclic cracking, creating very intensive shear bands. In fact, similar results have emerged in the on the machining of hard metals literature [26].

The schematic diagrams of the chip height ratio and serrated pitch measurement obtained as a result of both experimental and numerical work are shown in Figure 12. The chip deformation degree can be characterized by the chip height ratio (Gs) and the chip height ratio is calculated as given in Eq.2: [15]:

$$G_S = \frac{h_1 - h_2}{h_1} \quad (2)$$

where Gs is chip height ratio, h_1 is the height from the bottom of chip to the peak of serrated chip, and h_2 is the height from the bottom of chip to the lowest valley of serrated chip. The serrated pitch (Pc) can be obtained by measuring the distance between the addenda of two adjacent

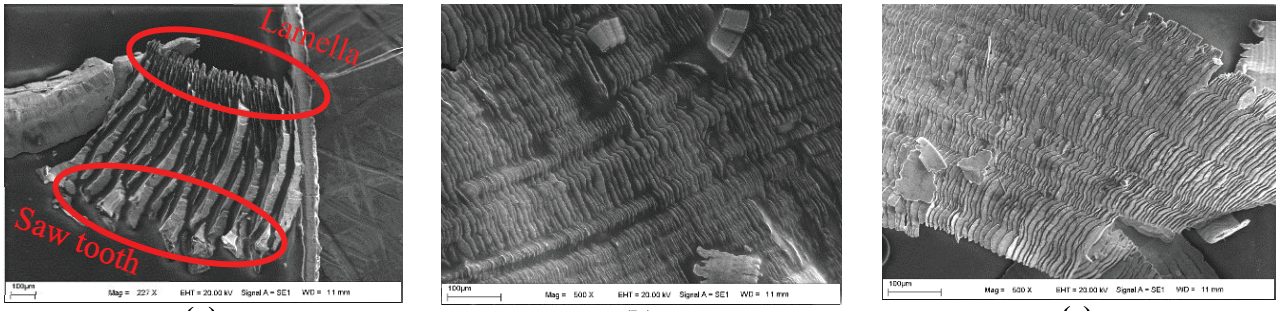

Figure 10. Lamella structure formation at; a) transition of saw teeth and lamella structure, b) 0.3 mm/rev, c) 0.2 mm/rev.

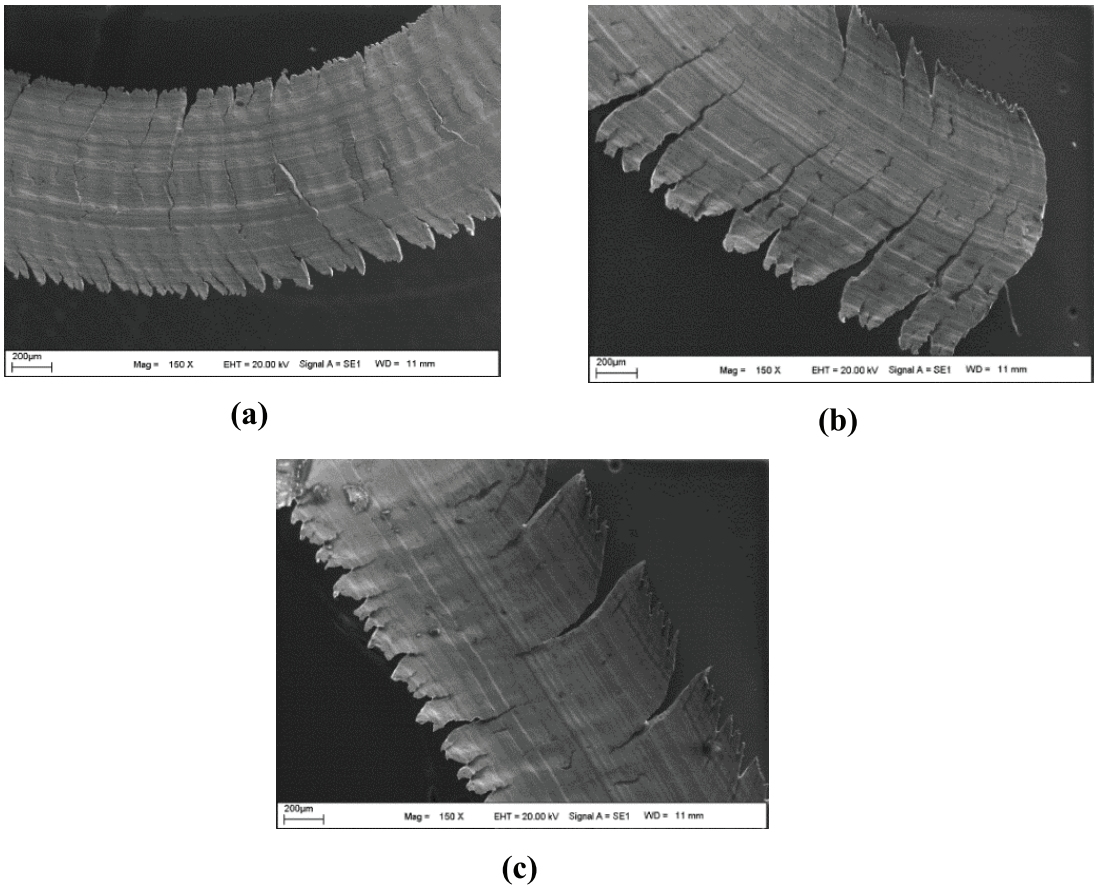

Figure 11. Chip morphology at varying feed rate; a) 0.1 mm/rev, b) 0.2 mm/rev, c) 0.3 mm/rev.

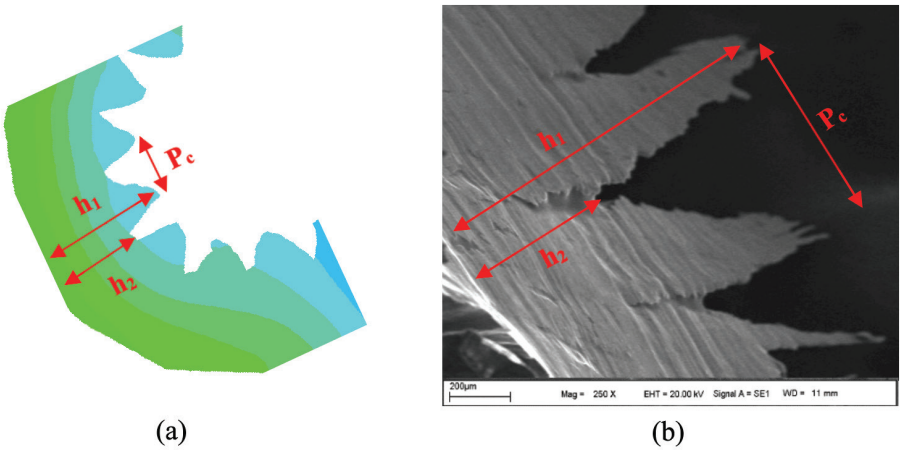

Figure 12. Comparison of modeled and experimental chip; a) modelled chip, b) experimental chip.

teeth in the chip. Each of the geometric characteristic parameters of the chip was measured 5 times and the average values of Gs and Pc were used.

In Figure 13, the chip height ratio and tooth pitch variation of the chips obtained from both experimental and numerical analyses at different feed rates are given. When the change in the tooth height ratios is examined, this ratio decreases with an increase in the feed rate. With the increase of the feed rate, the cutting area between the tool and the cutting workpiece increases, which increases the chip pit height (h_2) while decreasing the chip top height (h_1). It was observed that it decreased by 31% at a feed rate of 0.2 mm/

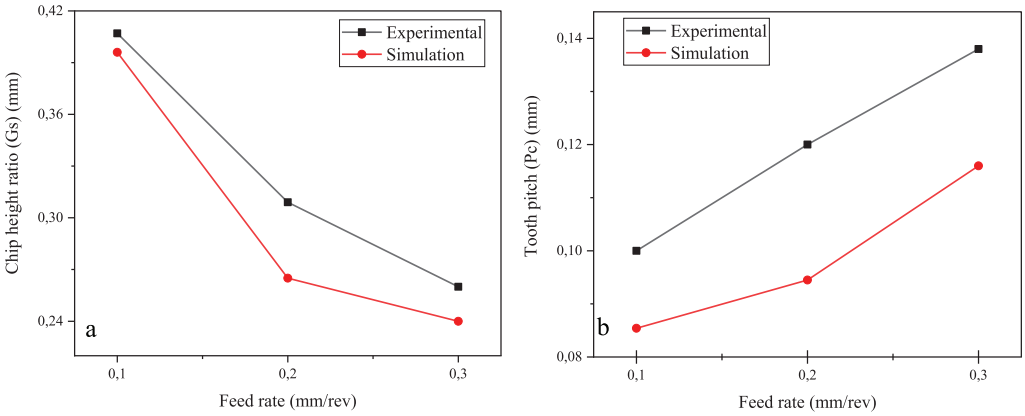

Figure 13. Comparison of saw-tooth degree of modeled and experimental chip; a) chip height ratio, b) tooth pitch.

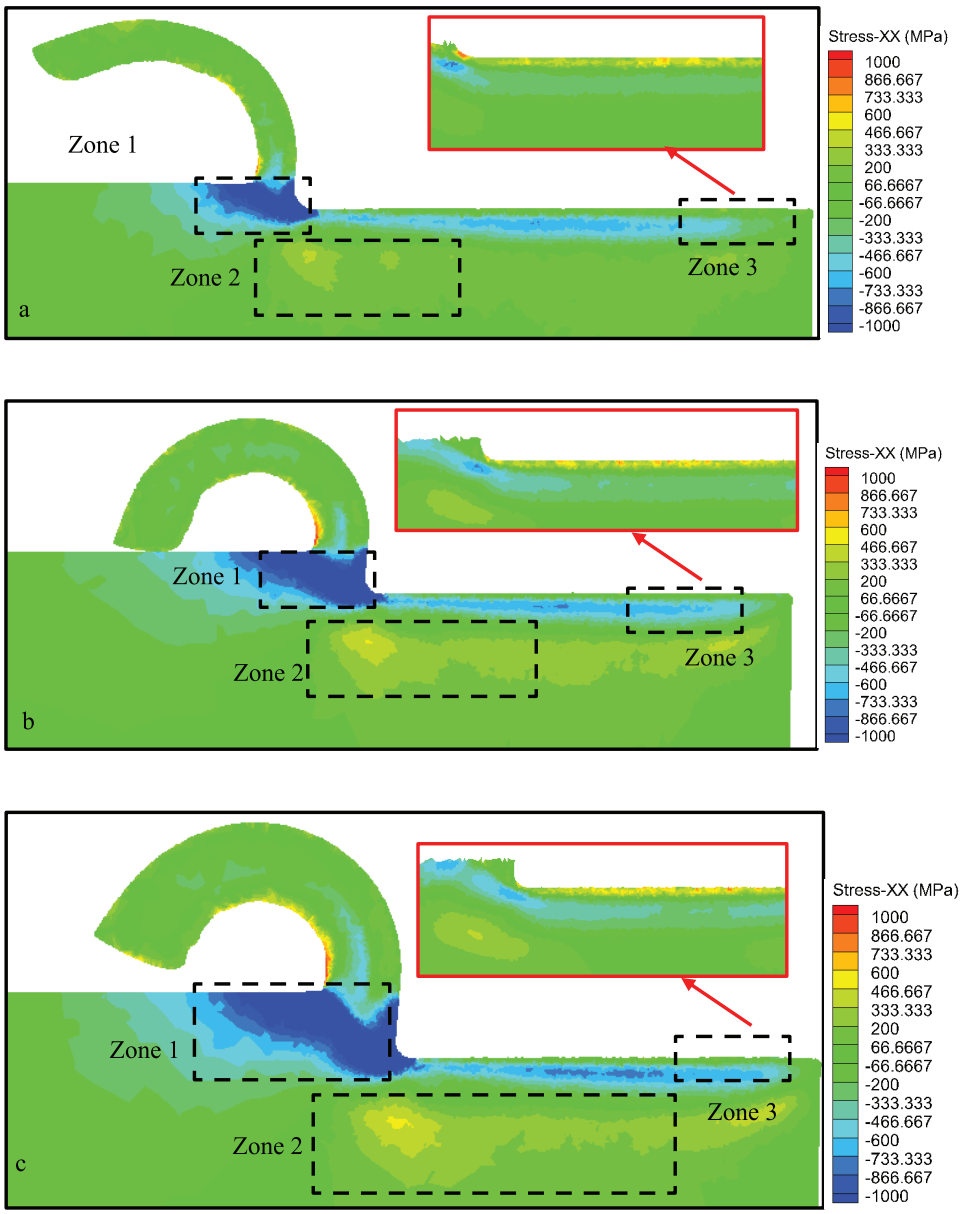

Figure 14. Formation mechanism of residual stress; a) f=0.1 mm/rev, b) f=0.2 mm/rev, c) f=0.3 mm/rev

rev compared to a feed rate of 0.1 mm/rev, and by 20% at a feed rate of 0.3 mm/rev compared to a feed rate of 0.2 mm/rev. Conversely, the tooth pitch values increase with the increase in the feed rate. It was observed that it increased 20% at 0.2 mm/rev feed rate compared to 0.1 mm/rev feed rate, and 15% increased at 0.3 mm/rev feed rate compared to 0.2 mm/rev feed rate. In fact, similar results have been observed in studies focused on the investigation of chip morphology by researchers in the literature [27,28].

Residual Stress

The variation of the simulated residual stress along the depth of the workpiece at various feed rates was analyzed, as shown in Figure 14. The maximum compressive residual stress was observed on the machined surface. Three stress zones occurred as a result of the contact between the tool and the workpiece. Zone 1 was formed in front of the cutting edge, and less tensile stress occurred in zone 2 compared to zone 1. The stress occurring in this region was in the opposite direction to the shear plane. Zone 3 occurred on the surface and lower layers of the workpiece, and especially in this region, there was a mechanical load accumulation. It was also greatly affected by the thermal load in this region, as heat generation occurred due to plastic deformation during chip removal and friction between the tool and the workpiece. However, the heat gradient formed on the surface was limited by the subsurface layers, thus compressive plastic stress occurred in the surface layer.

Tool Wear

During the machining of Co alloys, crater wear, lower tungsten particles stick between the workpiece and the cutting tool, also high levels of diffusion speeds occur [29]. In this study, after the machining of CoCrMo alloy, microscopic images were taken from carbide cutting tool at 3 different feed rates (0.1, 0.2, 0.3 mm/rev) at the of

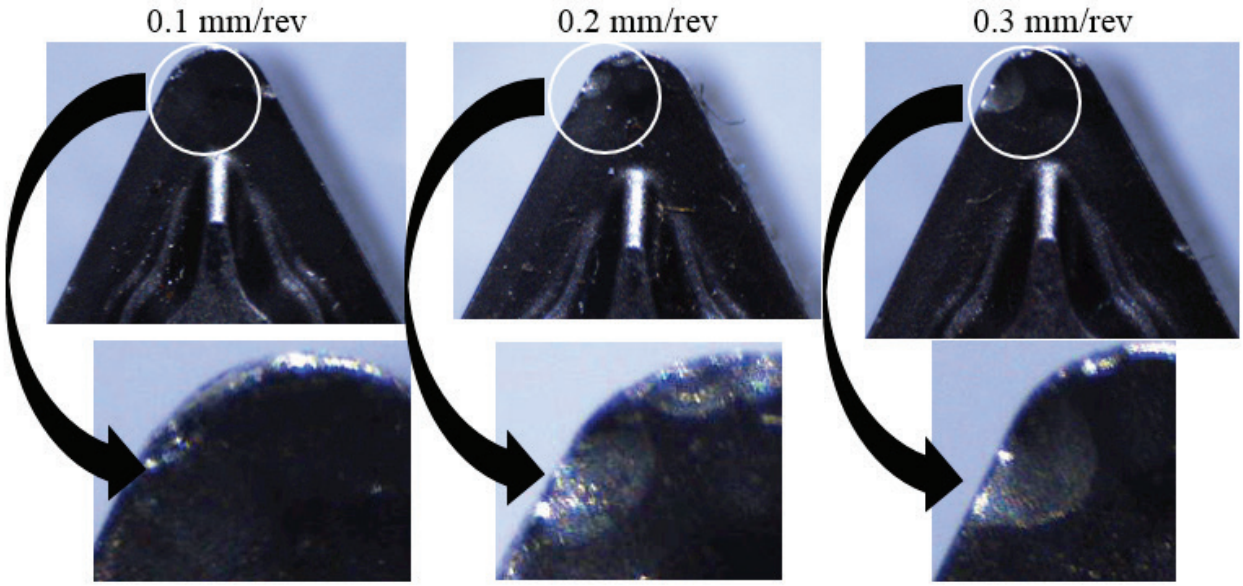

Figure 15. Change of crater wear dimensions due to increased feed rate.

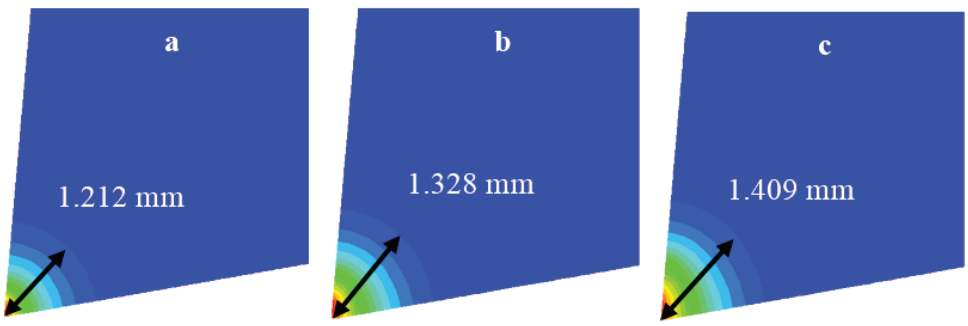

Figure 16. Distribution of temperature influence area due to increase in progress; a) 0.1 mm/rev, b) 0.2 mm/rev, c) 0.3 mm/rev.

Table 4. Change of crater wear area according to feedrate

Feed rate (mm/rev)	0.1	0.2	0.3
Crater wear area (mm^2)	0.9935	2.27	3.56

manufacturing. Microscop images showed a significant increase in the progression of tool wear. Images showed a significant increase in crater sizes due to the increase in progression at a constant 80 m/min (Figure 15). Increasing the feed rate during production increases the amount of chips removed per unit time, which in turn leads to an increase in the temperature between the workpiece and the cutting tool [30-32]. Thus, the size of the crater wear gradually increases. Table 4 gives the measurement results of the wear areas that occur in the cutting tool. The values support the microscopic images. Furthermore, from the FEM analysis, with the increase of the progression on the cutting tool (Figure 16). It was seen that the effect area of the temperature increased significantly. As a result of the analysis, it was seen that the temperature formed at 0.1 mm/rev advance was approximately significant to 1.212 mm distance from the tool tip, 1.328 mm distance at 0.2 mm/rev and 1.409

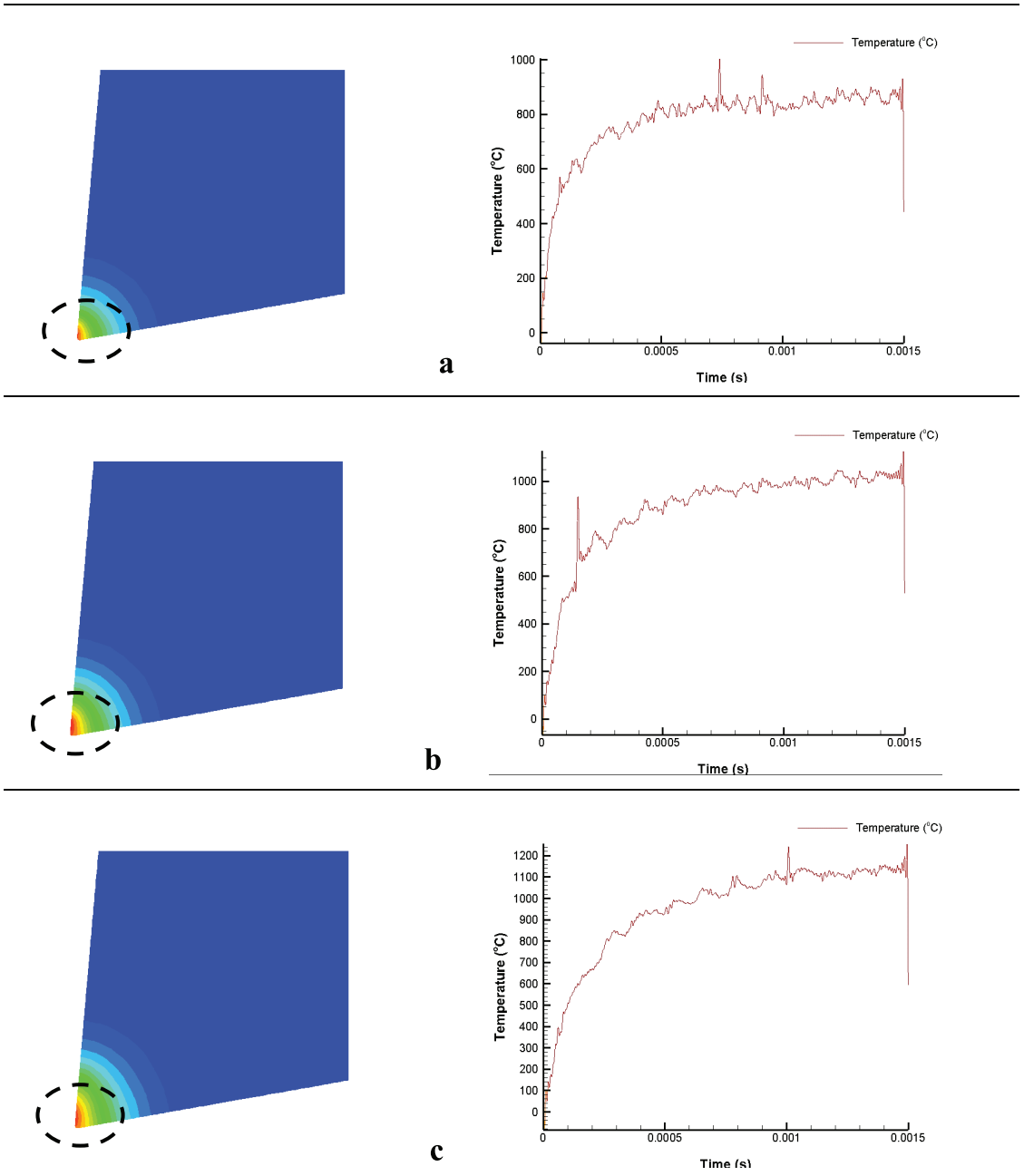

Figure 17. Peak temperature change in the tool at different feed rates; a) 0.1 mm/rev, b) 0.2 mm/rev, c) 0.3 mm/rev.

mm distance at 0.3 mm/rev feed rate. Additionally, the peak temperature changes that occurred during the manufacturing process of the cutting tool were examined (Figure 17). The highest feedrate used in the analyses was increased to 1200°C with a maximum peak temperature of 0.3 mm/rev. While the other feed rates increased to a maximum of 1000°C. Thus, it was observed that the high temperature values were directly associated with each other during crater wear and chip removal.

On the other hand, it has been observed that the interaction between the tool nose radius and the feed rate affects the tool wear area. The increase in the cutting zone temperature with the increase in feed rate did not significantly affect the tool nose radius. It has been found that the maximum temperature occurs in the middle of the tool-chip contact length and in the interaction of the corner radius of the tool with the side face. As a matter of fact, similar results were obtained in studies on the tool nose radius of machining parameters [33].

CONCLUSION

This article provides information about the results of the work performed by both experimental and numerical analyses of chip morphology and tool wear. The results obtained are as follows:

1. As a result of the FEM analysis, it was seen that the force that occurred with the increase of the feed rate in the force change results obtained during machining according to the orthogonal cutting model increased. The increase in the amount of chip to be removed per unit feed causes an increase in the force. Especially considering the force variation range, it is higher at a feed rate of 0.3 mm/rev than at a feed rates of 0.2 and 0.1 mm/rev.
2. Cracks and adhesion occurred due to the increase in the feed rate in the chip images examined by SEM. Smooth chip surfaces were obtained at a feed rate of 0.1 mm/rev. Cracks and adhesions were observed in the chip images at 0.2 and 0.3 mm/rev feed rates.
3. According to the experimental measurement and FEM analysis results, ASTM F75 CoCrMo alloy produces serrated chips regardless of the feed rate. However, with the increase in the feed rate, the serrated chip became more pronounced. As the feed rate increased, the Gs ratio decreased, while the Pc increased. Depending on the increase in the feed rate, the chip height ratio decreased by approximately 45% and the serrated pitch distance increased by 29%.
4. It was observed that the crater wear area increased with the increase in the feed rate. On the other hand, no significant change was observed in the tool nose radius due to the increase in the feed rate, as the maximum temperature occurred in the middle of the tool-chip contact length.

AUTHORSHIP CONTRIBUTIONS

Authors equally contributed to this work.

DATA AVAILABILITY STATEMENT

The authors confirm that the data that supports the findings of this study are available within the article. Raw data that support the finding of this study are available from the corresponding author, upon reasonable request.

CONFLICT OF INTEREST

The author declared no potential conflicts of interest with respect to the research, authorship, and/or publication of this article.

ETHICS

There are no ethical issues with the publication of this manuscript.

REFERENCES

[1] Attanasio A, Ceretti E, Fiorentino A, Cappellini C. Investigation and FEM-based simulation of tool wear in turning operations with uncoated carbide tools. Wear 2010;269:344–350. [CrossRef]

[2] Attanasio A, Faini F, Outeiro JC. FEM simulation of tool wear in drilling. Procedia CIRP 2017;58:440–444. [CrossRef]

[3] Gao XJ, Li H, Liu Q, Zou P, Liu F. Simulation of stainless steel drilling mechanism based on deform-3D. Adv Mater Res 2010;160-162:1685–1690. [CrossRef]

[4] Parida AK, Maity K. FEM analysis and experimental investigation of force and chip formation on hot turning of Inconel 625. Def Technol 2019;15:853–860. [CrossRef]

[5] Tang L, Sun Y, Li B, Sehn J, Meng G. Wear performance and mechanisms of PCBN tool in dry hard turning of AISI D2 hardened steel. Tribol Int 2019;132:228–236. [CrossRef]

[6] Li A. A review of tool wear estimation using theoretical analysis and numerical simulation technologies. Int J of Refract Met Hard Mater 2012;35:143–151. [CrossRef]

[7] Calamaz M, Limido J, Nouari M, Espinosa C, Coupard D, Salaün M, et al. Toward a better understanding of tool wear effect through a comparison between experiments and SPH numerical modelling of machining hard materials. Int J of Refract Met Hard Mater 2009;27:595–604. [CrossRef]

[8] Kountanya R, Al-Zkeri I, Altan T. Effect of tool edge geometry and cutting conditions on experimental and simulated chip morphology in orthogonal hard turning of 100Cr6 steel. J Mater Process Technol 2009;209:5068–5076. [CrossRef]

[9] Nan X, Xie L, Zhao W. On the application of 3D finite element modeling for small-diameter hole drilling of AISI 1045 steel.Int J Adv Manuf Technol 2015;84:1927–1939. [CrossRef]

[10] Yaylacı M, Abanoz M, Yaylacı EU, Ölmez H, Sekban DM, Birinci A. Evaluation of the contact problem of functionally graded layer resting on rigid foundation pressed via rigid punch by analytical and numerical (FEM and MLP) methods. Arch App Mech 2022;92:1953–1971. [CrossRef]

[11] Adıyaman G, Birinci A, Öner E, Yaylacı MA. Receding contact problem between a functionally graded layer and two homogeneous quarter planes. Acta Mech 2016;227:1753–1766. [CrossRef]

[12] Zhang G, To S, Xiao G. The relation between chip morphology and tool wear in ultra-precision raster milling. Int J Mach Tools Manuf 2014;80-81:11–17. [CrossRef]

[13] Jagtap KA, Pawade RS. Some studies on chip formation mechanism in CNC turning of biocompatible Co-Cr-Mo alloy. Procedia Manuf 2018;20:283–289. [CrossRef]

[14] Parida AK, Maity K. Experimental investigation on tool life and chip morphology in hot machining of Monel-400. Eng Sci Technol Int J 2018;21:371–379. [CrossRef]

[15] Zhao W, Gong L, Ren F, Li L, Xu Q, Khan AM. Experimental study on chip deformation of Ti-6Al-4V titanium alloy in cryogenic cutting. Int J Adv Manuf Technol 2018;96:4021–4027. [CrossRef]

[16] Bolat Ç, Ergene B, Karakılınç U, Gökşenli A. Investigating on the machinability assessment of precision machining pumice reinforced AA7075 syntactic foam. J Mech Eng Sci 2021;236:1986–1996. [CrossRef]

[17] Alina BP, Aurel M. Study about the chip formation in the turning process using the finite element analysis,. The 25th Edition of IManEE 2021 International Conference (IManEE 2021) Mater Sci Eng 2022;1235:012019. [CrossRef]

[18] Wakjira MW, Janaki RP. Analysis of turning chip morphology with various tool geometries using finite element modeling and simulation to optimize product sustainability. Adv Mech Eng 2022;14:168781322211364. [CrossRef]

[19] Okokpujie IP, Chima PC, Tartibu LK. Experimental and 3D-deform finite element analysis on tool wear during turning of Al-Si-Mg alloy. Lubricants 2022;10:341. [CrossRef]

[20] Guoi Z, Pang X, Yan Y, Gao K, Volinsky AA, Zhang TY. CoCrMo alloy for orthopedic implant application enhanced corrosion and tribocorrosion properties by nitrogen ion implantation. Appl Surf Sci 2015;347:23–34. [CrossRef]

[21] Henriques B, Bagheri A, Gasik M, Souza JCM, Carvalho O, Silva FS, et al. Mechanical properties of hot pressed CoCrMo alloy compacts for biomedical applications. Mater Design 2015;83:829–834. [CrossRef]

[22] Nurulamin AKM, Jaafar IH, Patwarı AU, Zubaire WWD. Role of discrete nature of chip formation and natural vibrations of system components in chatter formation during metal cutting. IIUM Eng J 2010;11:124–138. [CrossRef]

[23] Rahman MA, Bhuiyan MS, Sharma S, Kamal MS, Imtiaz MMM, Alfaify A, et al. Influence of Feed Rate Response (FRR) on chip formation in micro and macro machining of AI alloy. Metals 2021;11:159. [CrossRef]

[24] Lee WB, Cheung CF, To S. A microplasticity analysis of micro-cutting force variation in ultra-precision diamond turning. J Manuf Sci Eng 2002;124:170–177. [CrossRef]

[25] Zhu Z, Guo K, Sun J, Li J, Liu Y, Chen L, et al. Evolution of 3D chip morphology and phase transformation in dry drilling Ti6Al4V alloys. J Manuf Process 2018;34:531–539. [CrossRef]

[26] M'Hamdi M, BenSalem S, Boujelbene M, Katundi D, Bayraktar E. Effect of cutting parameters on the chip formation in orthogonal cutting. AIP Conf Proc 2011;1315:1101–1106. [CrossRef]

[27] Li J, Tao Z, Cai X, An Q, Chen M. Experimental and finite element analysis of the formation mechanism of serrated chips of nickel-based superalloy Inconel 718. Int J Adv Manuf Tech 2020;107:4969–4982. [CrossRef]

[28] Singh BK, Roy H, Mondal B, Roy SS, Mandal N. Measurement of chip morphology and multi criteria optimization of turning parameters for machining of AISI 4340 steel using Y-ZTA cutting insert. Measurement 2019;142:181–194. [CrossRef]

[29] Bordin A, Bruschi S, Ghiotti A, Bariani PF. Analysis of tool wear in cryogenic machining of additive manufactured Ti6Al4V alloy. Wear 2015;328-329:89–99. [CrossRef]

[30] Alojali HM, Benyounis KY. Advances in Tool Wear in Turning Process. In: Hashmi, S, editor. Reference module in materials science and materials engineering. Amsterdam: Elsevier; 2015. [CrossRef]

[31] Balaji M, Venkata K, Mohan N, Murthy BSN. Optimization of drilling parameters for drilling of TI-6Al4V based on surface roughness, flank wear and drill vibration. Measurement 2018;114:332–339. [CrossRef]

[32] Grzesik W, Niesłony P, Habrat W, Sieniawski J, Laskowski P. Investigation of tool wear in the turning of Inconel 718 superalloy in terms of process performance and productivity enhancement. Tribol Int 2018;118:337–346. [CrossRef]

[33] Tagiuri ZAM, Dao TM, Samuel AM, Songmene V. A numerical model for predicting the effect of tool nose radius on machining process performance during orthogonal cutting of AISI 1045 steel. Materials (Basel) 2022;15:3369. [CrossRef]